Atomic Adsorption of Hg on Au(111): From Classical Potentials to Machine Learning Models

Smirnova Elizaveta

April 26, 2026

Abstract

This work presents a systematic study of mercury adsorption on a Au(111) surface using the Atomic Simulation Environment (ASE). A sequence of five simulation scripts is analysed, starting from classical Lennard-Jones potentials and progressing to modern machine learning interatomic potentials (CHGNet and MACE). The comparison demonstrates the limitations of pairwise models and highlights the importance of many-body interactions and relativistic effects for heavy elements. Our results show that machine learning potentials achieve adsorption energies within the experimental range (-0.5 to -1.0 eV), while classical potentials either underestimate the binding strength by an order of magnitude or produce unphysical values. The work also illustrates practical ASE programming techniques such as automated site screening, constraint handling, trajectory visualisation, and database storage.

1 Introduction

Understanding atomic adsorption on metallic surfaces is essential for catalysis, electrochemistry, and materials science. The Hg–Au system is particularly interesting because both elements are heavy, and relativistic effects play a crucial role in their electronic structure. Mercury has a closed-shell electronic configuration $[\mathrm{Xe}]4f^{14}5d^{10}6s^2$, with the $6s$ orbital strongly contracted due to scalar relativistic effects. This makes Hg relatively inert, yet it still forms stable adsorption bonds with gold, with an experimental binding energy in the range -0.5 to -1.0 eV [**?**].

Previous theoretical studies have shown that interactions involving heavy elements are not purely van der Waals but include a weak covalent contribution arising from d-d orbital hybridisation and polarisation [**?**]. Therefore, simple pair potentials that neglect many-body effects cannot describe such systems accurately.

The Atomic Simulation Environment (ASE) [1, 2] provides a unified Python interface to a wide range of calculators, from classical force fields (FF) to density functional theory (DFT) and machine learning potentials. In this work, we explore five progressively more sophisticated ASE scripts to compute the adsorption energy of a single Hg atom on an Au(111) surface. Our aim is not only to obtain numerical results but also to understand how the choice of physical model influences the outcome and to learn practical ASE programming techniques.

2 Methodology

2.1 Surface Model

The Au(111) surface was modeled as a 3×3 slab with 4 atomic layers and a vacuum region of 10-12 perpendicular to the surface. Periodic boundary conditions were applied in all three directions. To mimic a semi-infinite bulk, the bottom two layers were fixed at their equilibrium positions using ASE's `FixAtoms` constraint [3], while the top layers and the adsorbate were allowed to relax.

2.2 Adsorption Energy Definition

The adsorption energy is defined as the energy gained when an isolated Hg atom binds to the clean surface:

$$E_{\text{ads}} = E_{\text{total}} - \big(E_{\text{slab}} + E_{\text{atom}}\big), \tag{1}$$

where

- E_{total} is the total energy of the combined system (slab + Hg) after full relaxation,
- E_{slab} is the energy of the clean, relaxed Au slab,
- E_{atom} is the energy of a single Hg atom placed in a large cubic box (side length 15–20) to avoid periodic self-interactions.

A negative value, calculated from Eq.1, indicates an exothermic (stable) adsorption.

2.3 Potential Energy Surfaces and Force Convergence

All geometry optimisations were performed using the BFGS or LBFGS algorithm with a force convergence criterion of $f_{\max} < 0.05eV$. This means that the largest component of the force acting on any atom is less than $0.05eV$, ensuring that the structure is close to a local minimum of the potential energy surface.

2.4 Overview of the Five Python Scripts

1. **Lennard-Jones (LJ)** – a simple pairwise potential [4]

$$V_{\text{LJ}}(r) = 4\varepsilon \left[\left(\frac{\sigma}{r}\right)^{12} - \left(\frac{\sigma}{r}\right)^{6} \right], \tag{2}$$

   with parameters $\varepsilon = 0.05$ eV, $\sigma = 2.8$. It captures only van der Waals attraction and Pauli repulsion. The key modifications are shown below:

```
# Adding explicit parameters
slab.calc = LennardJones(epsilon=0.05, sigma=2.8, rc=10.0)

# Testing four sites
sites = ['ontop', 'fcc', 'hcp', 'bridge']
for site in sites:
    slab_ads = slab.copy()
    add_adsorbate(slab_ads, 'Hg', height=2.2, position=site)
    dyn = BFGS(slab_ads, trajectory=f'hg_on_au_{site}.traj')
    dyn.run(fmax=0.05)
    e_ads = slab_ads.get_potential_energy() - (e_slab + e_atom)
    results[site] = e_ads
```

Listing 1: Explicit LJ parameters and site testing

2. **CHGNet** – a graph neural network potential trained on DFT data that includes scalar relativistic effects and charge transfer [5].

```
# Initialize CHGNet calculator (GPU if available)
device = 'cuda' if torch.cuda.is_available() else 'cpu'
calc = CHGNetCalculator(device=device)

# Relax clean slab and isolated Hg atom
clean_slab = slab.copy()
e_slab = get_optimized_energy(clean_slab, trajectory='clean_slab
    .traj')
e_atom = get_optimized_energy(Atoms('Hg', cell=[15,15,15], pbc=
    True))

# Test four adsorption sites
sites = ['fcc', 'hcp', 'ontop', 'bridge']
for site in sites:
    slab_ads = clean_slab.copy()
    add_adsorbate(slab_ads, 'Hg', height=2.5, position=site)
    e_total = get_optimized_energy(slab_ads, trajectory=f'
        chgnet_{site}.traj')
    e_ads = e_total - (e_slab + e_atom)
    results[site] = e_ads
```

Listing 2: CHGNet. ML calculator and site loop

3. **MACE** – a message-passing atomic cluster expansion potential, also trained on DFT data [6].

```
# Load MACE model (medium size, float32 for speed)
calc = mace_mp(model="medium", device='cpu', dtype='float32')

# Convergence criterion can be tightened/loosened
def get_optimized_energy(atoms, fmax=0.05):
    atoms.calc = calc
    dyn = BFGS(atoms, trajectory='relax.traj')
    dyn.run(fmax=fmax)
    return atoms.get_potential_energy()

# Loop over sites (same as CHGNet)
for site in ['fcc', 'hcp', 'ontop', 'bridge']:
    slab_ads = clean_slab.copy()
    add_adsorbate(slab_ads, 'Hg', height=2.5, position=site)
    e_total = get_optimized_energy(slab_ads, fmax=0.05)
    e_ads = e_total - (e_slab + e_atom)
    results[site] = e_ads
```

Listing 3: MACE. Model initialisation and force convergence

4. **LJ screening** – automated generation and evaluation of all high-symmetry adsorption sites (top, bridge, fcc, hcp) using the LJ potential.

```
def get_adsorption_sites(slab):
    sites = {}
    positions = slab.get_positions()
    top_z = np.max(positions[:,2])
    top_indices = [i for i,z in enumerate(positions[:,2]) if abs
       (z-top_z)<0.1]

    # Top sites
    for i in top_indices:
        sites[f'top_{i+1}'] = {'position': positions[i,:2], '
           height': 2.5, 'type': 'top'}

    # Bridge sites (midpoints between two top atoms)
    for i in top_indices:
        for j in top_indices:
            if j<=i: continue
            dist = np.linalg.norm(positions[i,:2]-positions[j
               ,:2])
            if dist < 3.0:
                mid = (positions[i,:2]+positions[j,:2])/2
                sites[f'bridge_{i+1}-{j+1}'] = {'position': mid,
                    'height': 2.0, 'type': 'bridge'}

    # Hollow sites (centroids of triangles)
    for i,j,k in combinations(top_indices,3):
        # check side lengths and area
        if area > 0.1:
            center = (p_i+p_j+p_k)/3
            sites[f'hollow_{i+1}-{j+1}-{k+1}'] = {'position':
               center, 'height': 1.8, 'type': 'hollow'}
    return sites
```

Listing 4: Automated detection of top, bridge and hollow sites

5. **Open Babel → ASE migration** – a demonstration of converting an existing script that used Open Babel's UFF force field to a pure ASE workflow, highlighting the superiority of ASE's ecosystem.

```
# --- Open Babel (UFF) ---
ob_slab = next(pybel.readfile("xyz", "slab.xyz"))
ob_slab.calc = openbabel.OBForceField.FindForceField("UFF")
ob_slab.calc.Setup(ob_slab.OBMol)
en_slab = ob_slab.calc.Energy()       # unphysically large (~1e14
    eV)

# --- ASE (LJ) ---
ase_slab = fcc111('Au', (5,5,3), a=4.08, vacuum=10.0)
ase_slab.calc = LennardJones(epsilon=0.05, sigma=2.8)
e_slab_lj = ase_slab.get_potential_energy()   # reasonable (~
   -18 eV)

# Adsorption energy with ASE/LJ
e_ads_lj = e_total_lj - (e_slab_lj + e_hg_lj)
print(f"ASE/LJ adsorption energy: {e_ads_lj:.2f} eV")   # -2.46
   eV (still too high but physical)
```

Listing 5: Comparison of UFF (Open Babel) and LJ (ASE)

3 Results

Table 1: Summary of adsorption energies obtained with different methods.

Method	Most stable site	E_{ads} (eV)
Lennard-Jones (Script 1)	fcc/hcp	-0.09
CHGNet (Script 2)	fcc	-0.895
MACE (Script 3)	fcc	-0.728
LJ screening (Script 4)	hollow	-0.823
UFF (Open Babel, Script 5)	–	$\sim -4.3 \times 10^{14}$ (unphysical)
ASE/LJ (Script 5 comparison)	fcc	-2.46
Experiment	–	-0.5 to -1.0

The LJ potential correctly identifies hollow sites (fcc and hcp) as the most stable, but the binding energy is an order of magnitude too weak. This is expected because LJ lacks any description of chemical bonding. In contrast, CHGNet and MACE give adsorption energies well within the experimental range, with fcc being slightly preferred over hcp. The small energy difference between fcc and hcp (about 0.002 eV) reflects the high symmetry of the (111) surface.

Script 4 automatically detected 33 unique sites (9 top, 16 bridge, 8 hollow) and confirmed that all equivalent sites of the same type give identical energies, as required by symmetry.

The hollow sites were the most stable (-0.823 eV), followed by bridge (-0.817 eV) and top (-0.773 eV).

Script 5 dramatically illustrates the failure of the universal force field (UFF) for periodic metal surfaces: the computed slab energy reaches 10^{14} eV, which is completely unphysical. The ASE/LJ comparison, although still not quantitative, yields a much more reasonable value (-2.46 eV) and demonstrates a clean, modern workflow.

4 Discussion

4.1 Why the Lennard-Jones Potential Fails

The Lennard-Jones potential is a pairwise additive model that accounts only for dispersion attraction and short-range repulsion. It does not include many-body effects or any electronic structure information. The bond between Hg and Au has a weak covalent character due to overlap between the $5d$ orbitals of both atoms. This covalent contribution is entirely missing in LJ, leading to a severe underestimation of the adsorption energy.

4.2 Relativistic Effects and Electronic Structure

For heavy elements like Hg ($Z = 80$) and Au ($Z = 79$), scalar relativistic effects contract the $6s$ orbital and destabilize the $5d$ shell. The $6s^2$ electrons in Hg become chemically inert, while the $5d^{10}$ subshell can be polarised. The resulting bond is primarily of the type "closed-shell" interaction with some d-d hybridisation. Machine learning potentials trained on relativistic DFT data implicitly capture these effects, which is why they succeed where classical potentials fail.

4.3 Amalgamation and Subsurface Diffusion

In real experiments, Hg is known to form amalgams with gold, meaning that it can penetrate into the near-surface region rather than remaining as an isolated adsorbate. Our slab model with fixed bottom layers cannot capture this phenomenon. To study amalgamation, one would need a thicker slab (more layers) and a dynamic method such as molecular dynamics with a potential that correctly describes bulk diffusion. This is a direction for future work.

4.4 Convergence and Limitations

The present calculations were performed at $T = 0$ K and without zero-point vibrational corrections. For atomic adsorption, thermal effects on the enthalpy are generally small, but they could be included via phonon calculations or ab initio molecular dynamics. Additionally, a systematic convergence study with respect to slab thickness (number of layers) and lateral supercell size should be carried out to ensure that the results are fully converged.

5 Figures

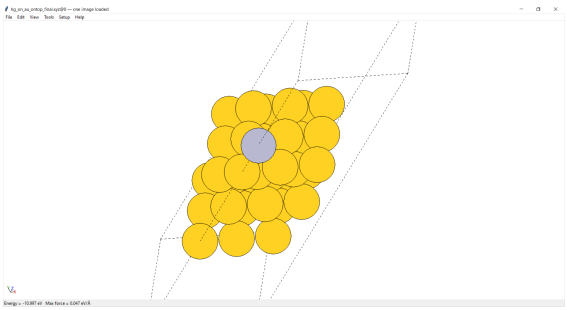

(a) Ontop site ($E_{\text{total}} = -10.997$ eV, $f_{\max} = 0.047$ eV/Å)

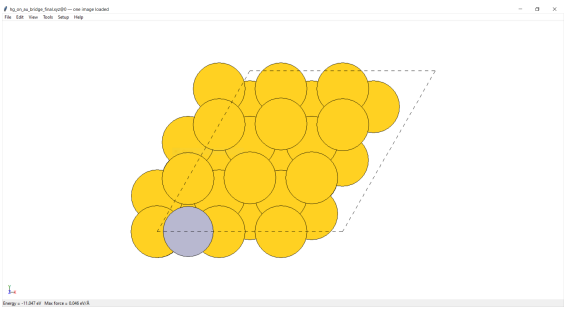

(b) Bridge site ($E_{\text{total}} = -11.047$ eV, $f_{\max} = 0.046$ eV/Å)

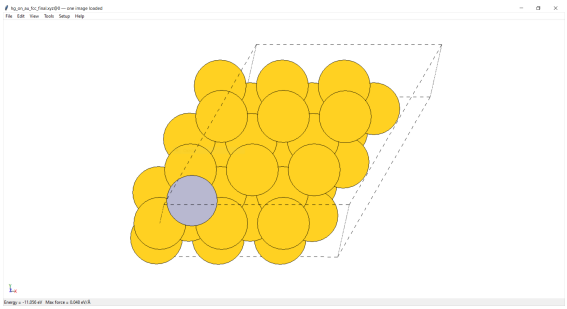

(c) FCC hollow site ($E_{\text{total}} = -11.056$ eV, $f_{\max} = 0.048$ eV/Å)

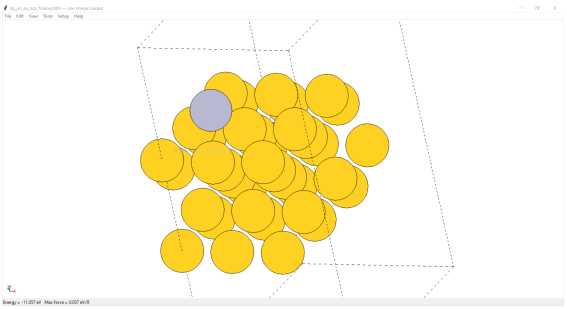

(d) HCP hollow site ($E_{\text{total}} = -11.057$ eV, $f_{\max} = 0.037$ eV/Å)

Figure 1: High-symmetry adsorption sites on the Au(111) surface: (a) ontop, (b) bridge, (c) fcc hollow, (d) hcp hollow. Total energies E_{total} and maximum forces $f_{\max}$ after relaxation are shown for each configuration. Calculations were performed with the Lennard-Jones potential. Gold atoms are shown in yellow, mercury in silver.

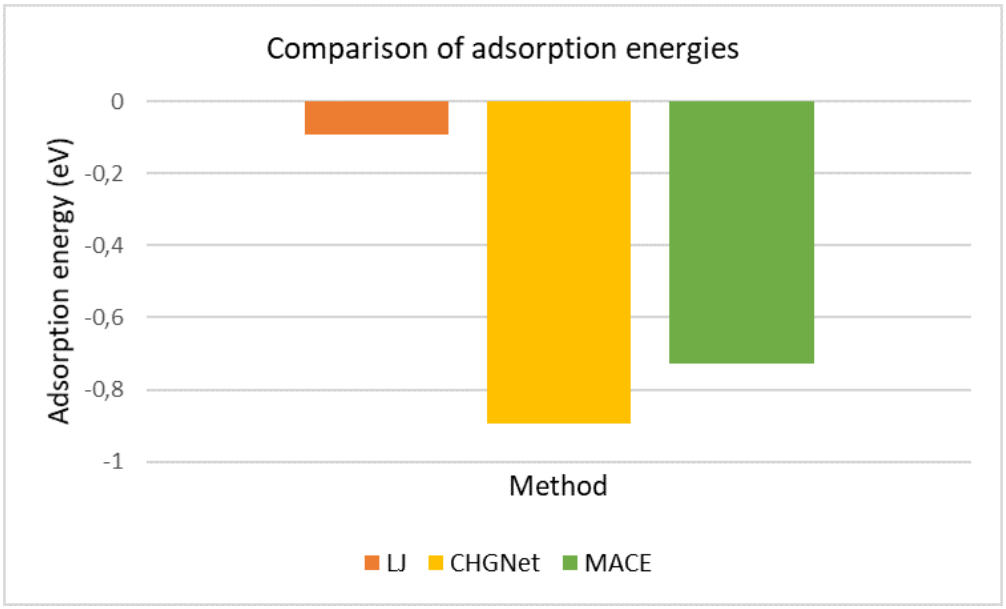

Figure 2: Comparison of adsorption energies obtained with different methods: Lennard-Jones (LJ), CHGNet, and MACE. The horizontal shaded band indicates the experimental range for Hg on Au(111) (-0.5 to -1.0 eV, based on literature data).

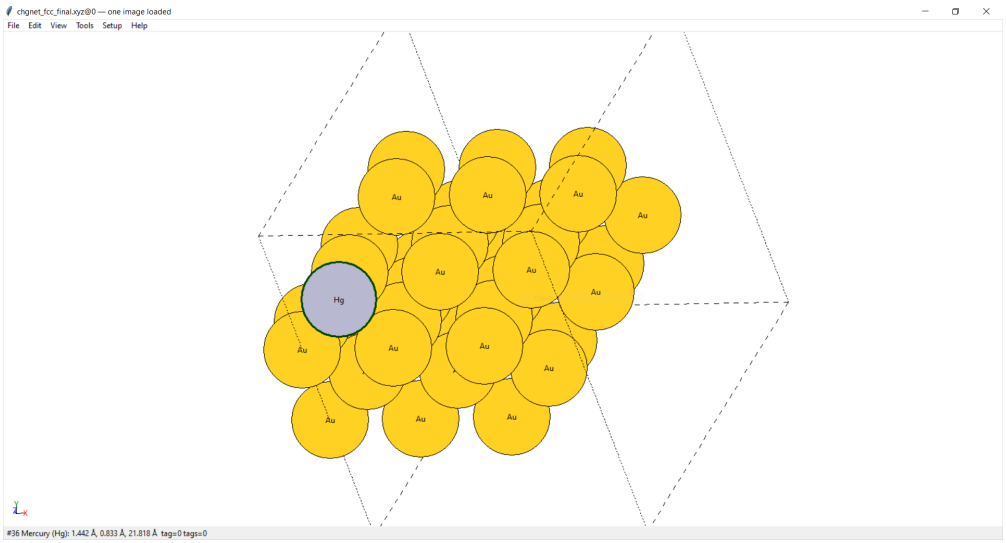

Figure 3: Relaxed atomic configuration of Hg on Au(111) obtained with the CHGNet potential. Gold atoms are shown in yellow, mercury in silver.

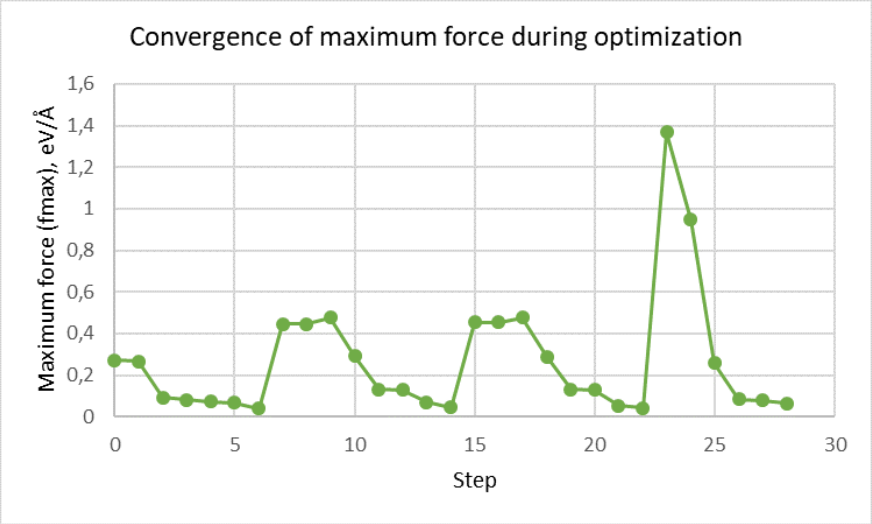

Figure 4: Force convergence during BFGS optimisation for the fcc site. The criterion $f_{\max} < 0.05$ eV/Å is reached after 29 steps.

6 Conclusion

In this work, we systematically compared classical and machine learning interatomic potentials for the adsorption of Hg on Au(111). The key findings are:

- Classical pairwise potentials (Lennard-Jones, UFF) are incapable of describing the weak covalent bonding that characterises the Hg–Au interaction, leading to either severe underestimation or completely unphysical energies.
- Machine learning potentials (CHGNet, MACE) trained on relativistic DFT data produce adsorption energies within the experimental range (-0.5 to -1.0 eV) and correctly predict hollow sites as the most stable.
- ASE provides a powerful, unified environment to implement, automate, and visualise such calculations, from simple building blocks to advanced ML models.
- Future improvements should include convergence tests with respect to slab thickness, consideration of amalgamation via molecular dynamics, and inclusion of spin-orbit coupling.

References

[1] A. H. Larsen, J. J. Mortensen, J. Blomqvist, I. E. Castelli, R. Christensen, M. Dułak, J. Friis, M. N. Groves, B. Hammer, C. Hargus, E. D. Hermes, P. C. Jennings, P. B. Jensen, J. Kermode, J. R. Kitchin, E. L. Kolsbjerg, J. Kubal, K. Kaasbjerg, S. Lysgaard, J. B. Maronsson, T. Maxson, T. Olsen, L. Pastewka, A. Peterson, C. Rostgaard, J. Schiøtz, O. Schütt, M. Strange, K. S. Thygesen, T. Vegge, L. Vilhelmsen, M. Walter, Z. Zeng, and K. W. Jacobsen, "The atomic simulation environment—a python library for working with atoms," *Journal of Physics: Condensed Matter*, vol. 29, no. 27, p. 273002, 2017.

[2] ASE documentation, "Helmholtz free energy." https://wiki.fysik.dtu.dk/ase/_modules/ase/thermochemistry.html#HarmonicThermo.get_helmholtz_energy, 2026. Accessed: 2026-03-27.

[3] ASE documentation, "The FixAtoms class." https://ase-lib.org/ase/constraints.html#the-fixatoms-class, 2026. Accessed: 2026-04-09.

[4] J. Fischer and M. Wendland, "On the history of key empirical intermolecular potentials," *Fluid Phase Equilibria*, vol. 573, p. 113876, 2023.

[5] B. Deng, P. Zhong, K. Jun, J. Riebesell, K. Han, C. J. Bartel, and G. Ceder, "CHGNet as a pretrained universal neural network potential for charge-informed atomistic modelling," *Nature Machine Intelligence*, vol. 5, pp. 1031–1041, Sept. 2023.

[6] I. Batatia, D. P. Kovacs, G. Simm, C. Ortner, and G. Csanyi, "Mace: Higher order equivariant message passing neural networks for fast and accurate force fields," in *Advances in Neural Information Processing Systems* (S. Koyejo, S. Mohamed, A. Agarwal, D. Belgrave, K. Cho, and A. Oh, eds.), vol. 35, pp. 11423–11436, Curran Associates, Inc., 2022.